ACADEMIC PRESS

Available online at www.sciencedirect.com

SCIENCE DIRECT®

Journal of Magnetic Resonance 162 (2003) 328–335

JMR Journal of Magnetic Resonance

www.elsevier.com/locate/jmr

The equivalence between off-resonance and on-resonance pulse sequences and its application to steady-state free precession with diffusion in inhomogeneous fields

D.E. Freed,* M.D. Hürlimann, and U.M. Scheven

Schlumberger-Doll Research, 36 Old Quarry Road, Ridgefield, CT 06877 USA

Received 8 October 2002; revised 22 January 2003

Abstract

We show that the spin dynamics of any pulse sequence with off-resonant pulses is identical to that of a modified sequence with on-resonant pulses, including relaxation and diffusion effects. This equivalence applies to pulse sequences with arbitrary offset frequency $\delta\omega_0$ which may exceed the RF field strength ω_1. Using this approach, we examine steady-state free precession (SSFP) in grossly inhomogeneous fields. We show explicitly that the magnitude of the magnetization for each mode at an offset frequency $\delta\omega_0$ is equal to that for SSFP with on-resonance pulses of rescaled amplitude, with the same dependence on relaxation times and diffusion coefficient. The rescaling depends on offset frequency and RF field strength. The theoretical results have been tested experimentally and excellent agreement is found.

1. Introduction

Nuclear magnetic resonance in grossly inhomogeneous fields is becoming increasingly of interest in applications ranging from NMR oil logging to medical imaging [1–5]. In extremely inhomogeneous fields, it is unavoidable that the RF frequency of RF pulses differs significantly from the Larmor frequency of most spins. Under such off-resonance conditions, precession during a pulse is important. This complicates the analysis of the response to pulse sequences in inhomogeneous fields. Various schemes for describing the effects of off-resonance RF pulses have been used in the literature, starting with the early work of Jaynes [6] and Bloom [7]. Our approach in this paper is based on the fact that any rotation around an arbitrary axis can be decomposed into a succession of three rotations around two orthogonal axes. In particular, the action of an arbitrary rotation can be described by an initial z-rotation of angle η, followed by a rotation of angle α_{eff} around an axis in the transverse plane, followed by a final z-rotation of angle η. The angles α_{eff} and η are closely related to the Euler angles. An off-resonance RF pulse is then equivalent to an on-resonance pulse with identical phase but new angle α_{eff}, preceded and followed by precessions of angle η. Therefore, for any pulse sequence with off-resonance pulses, there is an equivalent pulse sequence with on-resonance pulses that exhibits identical spin dynamics, including relaxation and diffusion behavior.

Demonstrating the efficacy of this equivalence, we consider the case of steady-state free precession (SSFP). This pulse sequence consists of a long string of identical pulses of nominal angle α, spaced apart by time T_R. After a time long compared to the relaxation time, the spins reach a dynamic equilibrium [8–10]. The magnetization in this dynamic equilibrium can be very sensitive to diffusion [11,12]. In a recent paper [13], we have analyzed in detail for on-resonance pulses the dependence of this equilibrium on diffusion, relaxation, pulse angle, and pulse spacing. Here we demonstrate both theoretically and experimentally that this analysis can be directly extended to situations with large off-resonance conditions using the general description of pulses indicated above. We show that the magnitude of the signal at an arbitrary offset frequency is equal to the on-reso-

* Corresponding author. Fax: 1-203-438-3819.
E-mail address: dfreed@ridgefield.oilfield.slb.com (D.E. Freed).

1090-7807/03/$ - see front matter © 2003 Elsevier Science (USA). All rights reserved.
doi:10.1016/S1090-7807(03)00041-7

nance response with a modified pulse angle, α_{eff}. In SSFP measurements, the pulse angle controls the relative importance of diffusion and relaxation effects [12,13]. This makes it possible to extract diffusion and relaxation information from a set of SSFP measurements with different pulse angles [10,12]. With an extended sample in a static gradient, the spectrum of a SSFP experiment yields simultaneous measurements on a continuum of angles α_{eff}. In this case, the original two-dimensional experiment can be replaced by a simple one-dimensional experiment.

In this paper we focus on the SSFP sequence for which the equivalence is particularly powerful. However, the method is applicable to all pulse sequences.

2. Rotations in inhomogeneous fields

In inhomogeneous B_0 fields, the RF frequency of the pulse and the Larmor frequency of the spins differ significantly for a large number of the spins. In a number of recent applications, NMR measurements have been performed in grossly inhomogeneous fields where the offset frequency, $\delta\omega_0$, can be much larger than the RF field strength, ω_1. In such cases, the precession during the pulses cannot be neglected. In a coordinate system where the z-axis is aligned with the static magnetic field, an x-pulse effectively rotates the magnetization about an axis $\hat{\boldsymbol{n}} = \frac{\omega_1}{\Omega}\hat{\boldsymbol{x}} + \frac{\delta\omega_0}{\Omega}\hat{\boldsymbol{z}}$ that is tipped out of the transverse plane, where the nutation frequency Ω is given by $\Omega = \sqrt{\omega_1^2 + \delta\omega_0^2}$.

It is advantageous to make use of a very general property of rotations to describe the effect of such off-resonance pulses. According to the description of the Euler angles, any rotation around an axis $\hat{\boldsymbol{n}}$ with an angle β can be described not only as a succession of rotations about the axes of the moving object, but also as a succession of rotations about axes in the stationary coordinate system [14]. This latter case is the one of interest here because the B_0 field selects out the z-axis. In this case, the first rotation is around the z-axis, the second around the x-axis and the third around the z-axis. Thus, a rotation with net angle β around an axis $\hat{\boldsymbol{n}}$ can be decomposed as follows:

$$R(\beta\hat{\boldsymbol{n}}) = R((\eta+\phi)\hat{z})R(\alpha_{\text{eff}}\hat{\boldsymbol{x}})R((\eta-\phi)\hat{z}). \tag{1}$$

Here $\eta+\phi$, α_{eff}, and $\eta-\phi$ are the three Euler angles, and ϕ is the angle between the x-axis and the projection of $\hat{\boldsymbol{n}}$ onto the x–y plane. The angles α_{eff} and η have the following interpretation. For a vector that starts out along the z-axis, the angle α_{eff} is the net amount the vector is tipped away from the z-axis by the rotation, and η is the net angle that its projection sweeps out in the transverse plane.Without loss of generality, we can set $\phi = 0$ and $\hat{\boldsymbol{n}} = n_x\hat{\boldsymbol{x}} + n_z\hat{\boldsymbol{z}}$. In that case, Eq. (1) reduces to

$$R(\beta\hat{\boldsymbol{n}}) = R(\eta\hat{z})R(\alpha_{\text{eff}}\hat{\boldsymbol{x}})R(\eta\hat{z}). \tag{2}$$

In terms of the angular momentum operator $\vec{I}$, this can be written as

$$e^{i\beta\vec{I}\cdot\hat{\boldsymbol{n}}} = e^{i\eta\vec{I}\cdot\hat{z}}e^{i\alpha_{\text{eff}}\vec{I}\cdot\hat{\boldsymbol{x}}}e^{i\eta\vec{I}\cdot\hat{z}}. \tag{3}$$

In these equations, the angle α_{eff} and the phase η are given by

$$\cos\alpha_{\text{eff}} = n_x^2\cos\beta + n_z^2, \tag{4}$$

with $0 \leqslant \alpha_{\text{eff}} \leqslant \pi$, and

$$\tan\eta = n_z\tan\frac{\beta}{2}, \tag{5}$$

with $|\eta| < \pi/2$ when $n_x\sin\beta/2 > 0$ and $\pi/2 < |\eta| < \pi$ when $n_x\sin\beta/2 < 0$. Eqs. 2–5 can be verified using the equations for the rotation matrix in [6] or by using the expression for the net axis and net angle of the product of three rotations, given in [15].

This decomposition of the rotation is particularly useful for the analysis of off-resonance NMR pulses. Eq. (2) shows that an off-resonance pulse with net angle β is equivalent to an on-resonance pulse of angle α_{eff} that is preceded and followed by precessions of angle η. In the usual case of rectangular RF pulses of strength $B_1 = \gamma\omega_1$ and duration τ_p, the expression for the effective pulse angle α_{eff} and precession angle η reduces to

$$\cos(\alpha_{\text{eff}}) = \cos(\Omega\tau_p) + \left(\frac{\delta\omega_0}{\Omega}\right)^2\left[1-\cos(\Omega\tau_p)\right], \tag{6}$$

$$\tan(\eta) = \frac{\delta\omega_0}{\Omega}\tan\left(\frac{\Omega\tau_p}{2}\right). \tag{7}$$

Fig. 1 shows the dependence of α_{eff} and η on the offset frequency, $\delta\omega_0$, and RF field strength, ω_1. Note that with the convention of $0 \leqslant \alpha_{\text{eff}} \leqslant \pi$, on resonance α_{eff} is given by $\alpha_{\text{eff}}(\delta\omega_0 = 0) = \omega_1\tau_p$ with $\eta = 0$ for tipping angles $\omega_1\tau_p$ between 0 and π. When the tipping angle is increased further, the expression for α_{eff} on resonance becomes $\alpha_{\text{eff}}(\delta\omega_0 = 0) = 2\pi - \omega_1\tau_p$ with $\eta = \pi$. With our definition, the phase η in Fig. 1b is discontinuous. However, at every discontinuity the phase factor jumps between 0 and $\pm\pi$ and the effective angle α_{eff} is zero or π. As a consequence, the full rotation given by Eq. (2) remains continuous. At a constant RF field strength and pulse duration, the effective angle α_{eff} can be varied by going off-resonance. Thus, in an inhomogeneous field, the magnetization for a range of values of α_{eff} can be obtained simultaneously. However, the full range of α_{eff} can only be reached when the on-resonance tipping angle $\omega_1\tau_p$ is equal to $(2n+1)\pi$. As shown below, there are interesting cases when the extra precession between the pulses only affects the overall phase of the signal. In such cases, the magnitude of the signal will be constant on each contour line of α_{eff}. Lastly, by varying $\delta\omega_0\tau_p$ for a fixed value of ω_1, all values of the phase η can be swept out for any value of $\omega_1\tau_p$.

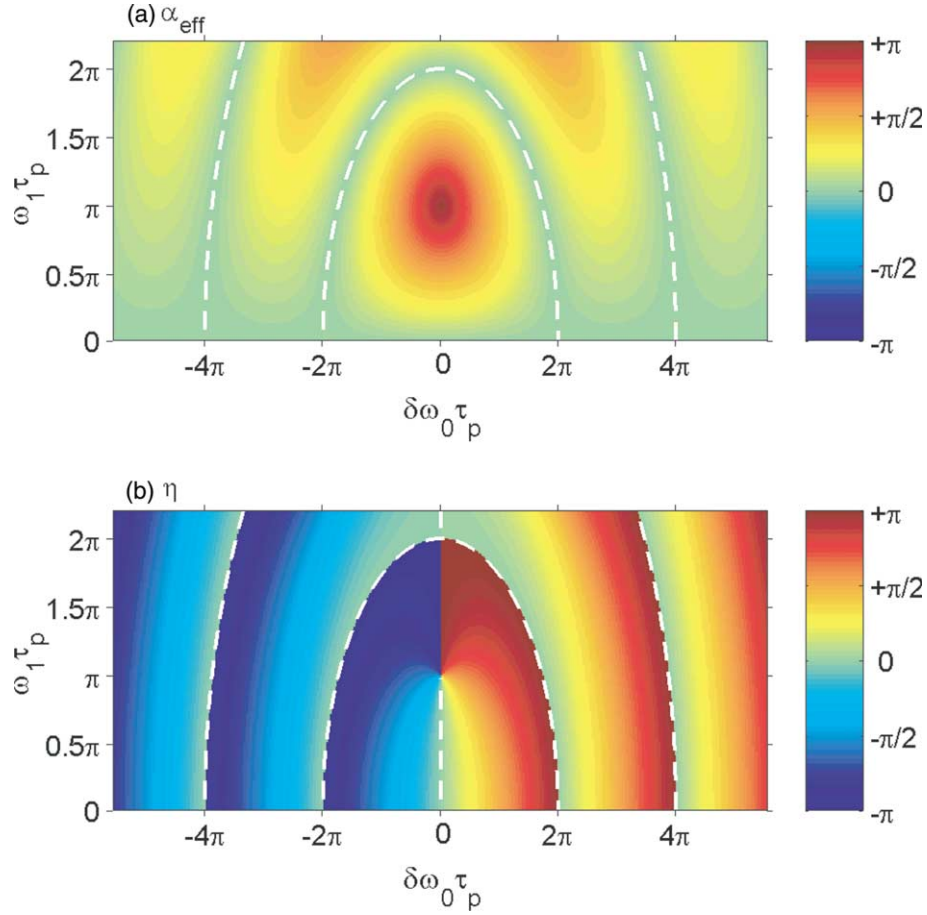

Fig. 1. (a) The effective angle α_{eff} as a function of normalized off-resonance frequency, $\delta\omega_0\tau_p$, and normalized RF field strength, $\omega_1\tau_p$. Contour lines for $\alpha_{\text{eff}} = 0$ are shown as dashed white lines. (b) The phase η as a function of $\delta\omega_0\tau_p$ and $\omega_1\tau_p$. Dashed white lines are contour lines for $\eta = 0$.

3. Solution for SSFP in inhomogeneous fields

3.1. Review of SSFP with near-resonance pulses

In [13] we have presented a detailed analysis of the SSFP signal for near-resonance pulses and discussed the dependence on diffusion, relaxation, and pulse spacing. This analysis is applicable to the case when the field inhomogeneity $\Delta\omega_0$ is small compared to the RF field strength, γB_1. In this section we use the decomposition of the off-resonance pulses to extend the previous SSFP results to fully include strong off-resonance effects. With this example, we demonstrate the utility of the decomposition of off-resonance pulses.

As in [10,13], we consider the dynamic equilibrium generated by a periodic stream of pulses of phase ϕ and pulse spacing T_R in the case of a static gradient g. The results extend easily to time varying gradients. We first summarize the results from [13] for near-resonance pulses: the magnetization between pulses can be expressed as a Fourier series in $\delta\omega_0$. For unrestricted diffusion, it has the form

$$M_x + iM_y = ie^{i\phi} \sum_p e^{i(p+t/T_R)\theta} b_p E_{2,p}(t), \tag{8}$$

where $\theta(\vec{r}) = \gamma \vec{g} \cdot \vec{r} T_R = \delta\omega_0 T_R$ is the average phase accumulated between pulses. The phase factor $ie^{i\phi}$ is uniform across the entire sample. Because it can be compensated by a constant phase shift, we will ignore it for the remainder of this section. The factor $E_{2,p}(t)$ describes the attenuation due to diffusion and relaxation for mode p. For spins with diffusion coefficient D and transverse relaxation time T_2, it is given by

$$E_{2,p}(t) = \exp\left(-t/T_2 - Dg^2\gamma^2 T_R^3 \left[p^2(t/T_R) + p(t/T_R)^2 + \frac{1}{3}(t/T_R)^3 \right] \right). \tag{9}$$

The different modes p are coupled by each RF pulse with an efficiency that depends on the pulse angle $\omega_1\tau_p$. The resulting mode amplitudes b_p of the dynamic equilibrium have to be calculated self-consistently. For near-resonance RF pulses, the amplitudes b_p are real and can be written in terms of a continued fraction. As explained

in [13], the solution of [10] in the presence of diffusion does not properly account for the coupling between modes. The diffusion sensitivity of the amplitudes b_p falls into different regimes [13] depending on the flip angle, pulse spacing and relaxation times.

The phase factor for mode p, $e^{i(p+t/T_R)\theta}$, vanishes at time $t = -pT_R$. At these distinct times, the magnetization of the pth mode is uniform across the whole sample, even with a large range of Larmor frequencies, and an echo is formed. The in-phase echo amplitude for mode p in steady state is given by

$$M_p(-pT_R) = b_p E_{2,p}(-pT_R). \tag{10}$$

During the application of RF pulses, t is always between 0 and T_R and only the modes $p = 0$ corresponding to a free induction decay (FID) and $p = -1$ (pre-FID) are observable. However, the higher echoes, corresponding to the modes with $p \leqslant -2$ can be reached with a stopped SSFP experiment. In this procedure, a train of pulses is first applied until the spins reach dynamic equilibrium. Then the pulsing is stopped. At the end of the pulse train, the magnetization is described by Eq. (8). Distinct echoes, given by Eq. (10) with $p \leqslant 0$, will form at time $t = -pT_R$ after the sequence has stopped. As long as the field inhomogeneity is large compared to $1/T_R$ so that $T_2^* < T_R$, the echoes will be well separated in time. For highly homogeneous fields where $T_2^* > T_R$, instead the echoes will overlap, but phase cycling can be used to separate out the contributions from different nodes [16].

3.2. Extension to large off-resonance pulses

We can now extend the results of the previous section to the case when the pulses are off-resonance. The identity in Eq. (2) shows that off-resonance pulses can be replaced by on-resonance pulses with a modified tipping angle $\alpha_{\text{eff}}(\delta\omega_0)$, given by Eq. (4), and extra precessions of angle $\eta(\delta\omega_0)$, given by Eq. (5) before and after each pulse. The solution for SSFP with off-resonance pulses is therefore identical to the solution of SSFP with near-resonance pulses of modified tipping angle $\alpha_{\text{eff}}(\delta\omega_0)$, except that the phase term in Eq. (8) is modified. For steady-state free precession with off-resonance pulses, the average phase acquired between pulses increases from θ to $\theta + 2\eta$. To calculate the magnetization after the last pulse, we also have to include the extra phase factor $e^{i\eta}$ following the final effective rotation of α_{eff}. With these changes, the magnetization immediately after a pulse for SSFP with off-resonance pulses becomes

$$M_x + iM_y = ie^{i\phi} \sum_p e^{i(p+t/T_R)\theta} e^{i(2p+1)\eta} b_p(\alpha_{\text{eff}}) E_{2,p}(t). \tag{11}$$

As before, we will assume that the overall phase factor $ie^{i\phi}$ has been taken care of by a constant phase correction. In Eq. (11), the coefficients $b_p(\alpha_{\text{eff}})$ are the solutions for mode amplitudes with on-resonance pulses of tipping angle α_{eff} which have been determined in [13]. This demonstrates the benefit of using the decomposition of the off-resonance pulse, since the off-resonance problem can be directly mapped onto an on-resonance problem. In Eq. (11) the only dependence on the off-resonance frequency $\delta\omega_0$ is through the parameters θ, η, and α_{eff}.

The extra phase shift of 2η is equivalent to shifting the offset frequency $\delta\omega_0$ further by $2\eta/T_R$ or to shifting the frequency of the RF pulse by $-2\eta/T_R$. It can also be thought of as adding additional precession times of $\eta/\delta\omega_0$ immediately before and after each pulse. During these precessions, the effects of relaxation and diffusion are taken to be negligible.

Diffusion leads to temporal fluctuations of the offset frequency $\delta\omega_0$ for a given spin. Our solution properly takes into account the effect of the resulting fluctuations in the phase accumulated between the pulses. However, in the mode expansion of Eq. (11), we ignore the temporal fluctuations in η and α_{eff} and also neglect diffusion during the application of the RF pulses. These are valid approximations as long as the pulse width τ_p is much smaller than the spacing between the pulses T_R, and the distance diffused by spins in non-negligible coherent pathways is much less than $(\gamma g \tau_p)^{-1}$, the distance over which η and α_{eff} change significantly. We note that these approximations are not specific to SSFP. The general equivalence between off-resonance and on-resonance pulse sequences is valid only if these conditions on the pulse width, pulse spacing, and diffusion length are met.

Within these approximations, Eq. (11) shows that the SSFP magnetization from the pth mode with off-resonance pulses leads to echoes with an echo amplitude at time $t = -pT_R$ after the last pulse of

$$M_p(-pT_R) = e^{i(2p+1)\eta} b_p(\alpha_{\text{eff}}) E_{2,p}(-pT_R). \tag{12}$$

This expression demonstrates that for off-resonance pulses with nutation angle $\Omega\tau_p$ and offset frequency $\delta\omega_0$, the magnitude of each SSFP echo is identical to the magnitude of the corresponding echo for on-resonance pulses of nutation angle α_{eff} given by Eq. (4). Hence the dependence on diffusion and relaxation for the off-resonance and the equivalent on-resonance sequences are identical. Compared with the on-resonance case, the magnetization at the pth echo acquires a phase φ_p proportional to the phase η:

$$\varphi_p = (2p+1)\eta. \tag{13}$$

Because the phase η, given by Eq. (5), only depends on the pulse parameters $\delta\omega_0\tau_p$ and $\omega_1\tau_p$, both η and φ_p are independent of diffusion and relaxation.

4. Experimental procedure

To verify the theoretical analysis for off-resonance SSFP, we performed stopped steady-state free preces-

sion measurements with an experimental setup that is identical to that described in [13] and is briefly reviewed here. A sample of water, doped with $NiCl_2$ to reduce the relaxation times to $T_1 = T_2 = 48.1$ ms, was placed in the fringe field outside a superconducting magnet. The diffusion coefficient of the sample is $D = 2.3 \times 10^{-9}\,m^2/s$. At the center of the sample the magnetic field strength was 41.5 mT, corresponding to a Larmor frequency of

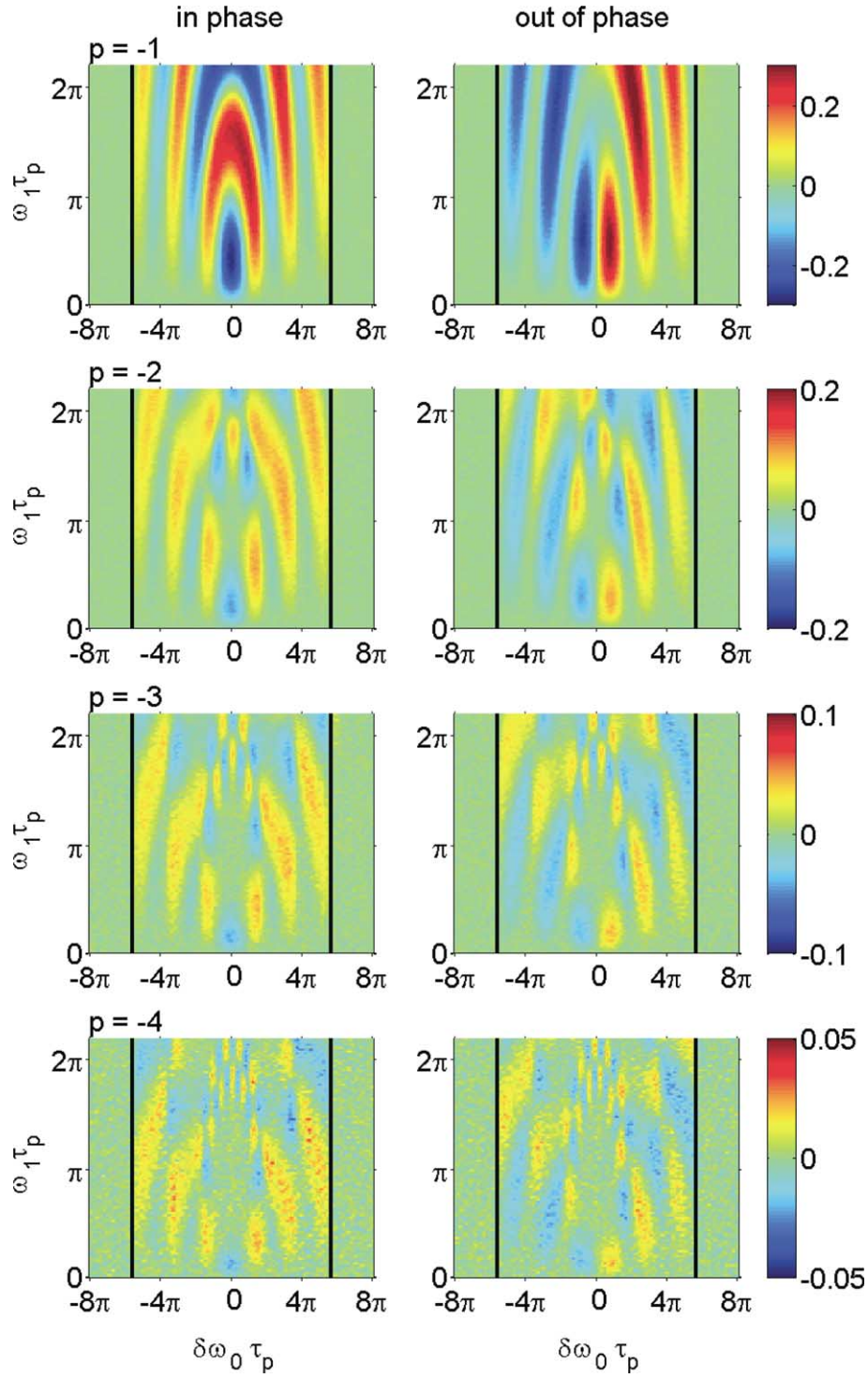

Fig. 2. Measured in-phase (left) and out-of-phase (right) spectra of the first four echoes of stopped steady-state-free-precession experiments in strongly inhomogeneous fields versus normalized off-resonance frequency, $\delta\omega_0\tau_p$ and normalized RF field strength, $\omega_1\tau_p$. From top to bottom, the four rows correspond to mode $p = -1, -2, -3$, and -4, respectively. The magnetization was normalized with respect to the thermal magnetization, M_0, and the color code for each mode is shown on the right. In these measurements, the pulse width was set to $\tau_p = 50\,\mu s$ and the pulse spacing to $T_R = 1$ ms. The black lines indicate the extent of the samples along the gradient direction.

1.76 MHz. The B_0 field variation across the cylindrical sample of 2 cm diameter and 2 cm height, that was oriented along the gradient direction, is well described by a uniform static gradient of 131 mT/m. Effects of RF inhomogeneities were minimized by using a comparatively large RF solenoid coil of 4 cm diameter and 10 cm length.

Stopped SSFP experiments were performed by applying trains of identical pulses for a duration of 160 ms $= 3.3T_1$, in which time the spins have reached steady state. At the end of the last pulse, we detected the first four echoes corresponding to the modes $p = -1$, -2, -3, and -4, respectively. In all measurements, the RF pulses were 50 μs long. Experiments were conducted for a range of RF amplitude settings corresponding to on-resonance flip angles $\omega_1\tau_p$ between 0 and 2.22π and for pulse spacings of 1, 2, 3, and 4 ms.

Separate experiments were performed to establish the value of the equilibrium magnetization M_0 and the relaxation time T_2 to better than 1% accuracy. The values of the flip angles were calibrated to limit the systematic error for the flip angles to less than two degrees.

In our experimental setup, the offset frequencies across the sample span ±55.8 kHz, corresponding to $\delta\omega_0\tau_p = \pm 5.6\pi$. The range of $\delta\omega_0$ is significantly larger than the RF field strength ω_1. Therefore, the echoes are well separated in time and have a width of the order of the pulse duration τ_p.

5. Comparison of experiment and theory

Fig. 2 shows the real and imaginary parts of experimental spectra of the first four echoes as a function of RF field strength $\omega_1\tau_p$. In these stopped SSFP experiments the pulse spacing was set to $T_R = 1$ ms. In the Fourier transform we chose the origin of the time axis for the $|p|$th echo to be $|p|T_R + (|p| - 1)\tau_p$, which corresponds closely to the echo peak. An overall constant phase shift was applied to the spectra for each echo.

The data show a complicated dependence on $\delta\omega_0$ and ω_1 with significant off-resonance magnetization even for $\delta\omega_0 > \omega_1$. The finite size of the sample limits frequency offsets in the experiments to $|\delta\omega_0\tau_p| < 5.6\pi$, which is indicated by black lines. On resonance, the measured signal has only a real component, independent of the RF field strength. Off-resonance, the out-of-phase component becomes important. Close inspection indicates a slight asymmetry of the spectra with respect to $\delta\omega_0$. We attribute this to small B_1 inhomogeneities and to the frequency dependence of the thermal equilibrium magnetization and coil response that become more noticeable at the low Larmor frequencies used in our measurements. In the further analysis, we have eliminated this complication to first order by symmetrizing the magnitude of each spectrum with respect to $\delta\omega_0$.

According to Eq. (12), the magnitude of the $|p|$th echo amplitudes shown in Fig. 2 depends on $\delta\omega_0$ and ω_1 only through $\alpha_{\text{eff}}(\delta\omega_0, \omega_1)$ introduced in Eq. (4). Similarly, the phase of the $|p|$th echo at time $|p|T_R$ depends on $\delta\omega_0$ and ω_1 only through $\eta(\delta\omega_0, \omega_1)$ introduced in Eq. (5). By changing the variables from $\delta\omega_0$ and ω_1 to the angles α_{eff} and η, the data of Fig. 2 should collapse onto single curves.

This is confirmed in Fig. 3. In the left-hand column, we have plotted the measured magnitudes of the echo amplitudes versus α_{eff} for the first four echoes. In the

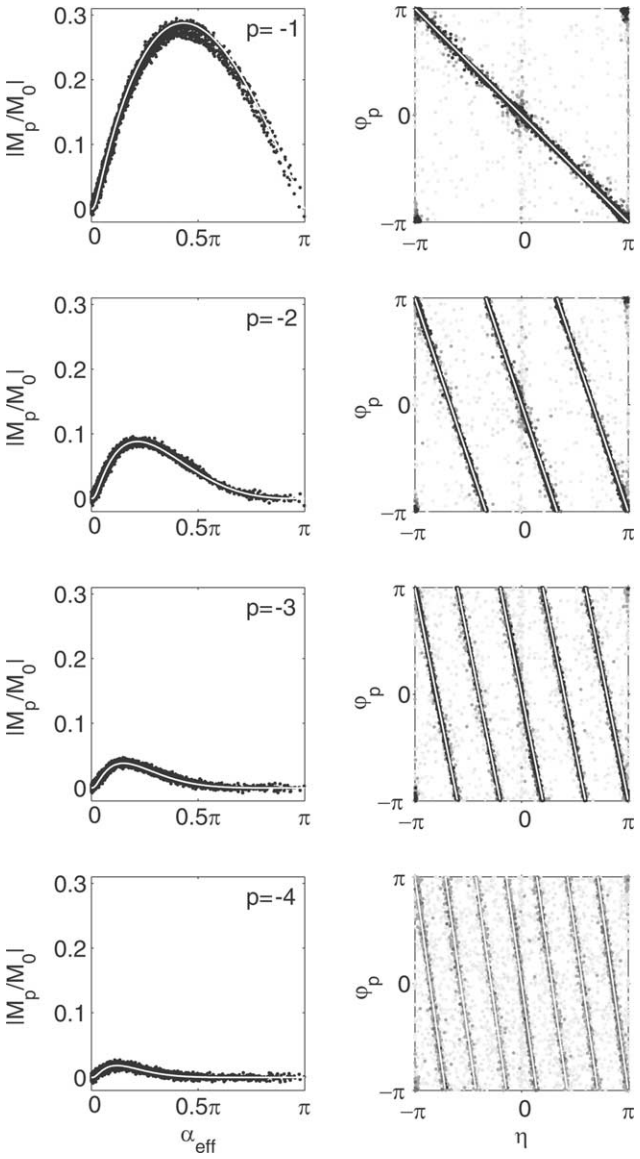

Fig. 3. Data collapse for the data shown in Fig. 2. In the left-hand column, the magnitudes of the signals normalized with respect to the thermal magnetization, M_0, are plotted as a function of α_{eff}. In the right-hand column, the phases at $t = |p|T_R$, φ_p, are plotted as a function of η. As in Fig. 2, results in rows 1–4 correspond to the first four echoes with $p = -1, -2, -3$, and -4, respectively. In the phase plots, the intensity of each point is weighted by the signal magnitude. Theoretical curves are plotted as solid white lines.

right-hand column, the measured phases φ_p at time $|p|T_R$ are plotted versus η. All the data of Fig. 2 with $|\delta\omega_0\tau_p| < 5.47\pi$ are included.

The data collapses in Fig. 3 are excellent for both the magnitude and phase and for all echoes. In addition to the collapses, the data are in full agreement with the theoretical predictions shown as solid white lines in Fig. 3. The measured phase φ_p for the $|p|$th echo is well described by $(2p+1)\eta$, independent of relaxation and diffusion. The magnitude of the $|p|$th echo is given by $|b_p|(\alpha_{\text{eff}})E_{2,p}(-pT_R)$. The white lines for the magnitudes are based on the solutions for b_p found in [13] with on-resonance pulses of tipping angle $\omega_1\tau_p = \alpha_{\text{eff}}$. The finite widths of the experimental curves for the magnitudes are systematic and are caused primarily by residual B_1 inhomogeneities.

Lastly, we demonstrate experimentally that the theoretical description of off-resonant pulses applies even in the presence of significant diffusion effects. As shown in [13], when the pulse spacing T_R is increased beyond $1/(\gamma g\sqrt{DT_2}) = 2.7\,\text{ms}$, diffusion effects become important and lead to a decrease in signal. In Fig. 4 we show the data collapses for the magnitudes of the first few echoes for stopped SSFP with four different pulse spacings and the comparisons with the theoretical results obtained with on-resonance pulses. In every case, the data for a given echo collapse to a single curve that is in agreement with the theoretical curve shown by the solid line. As can be seen in the figure, the magnitude of the echoes falls off significantly as the echo spacing is increased and diffusion effects become important. In contrast, the results for the phases are unaffected by diffusion and are identical to Fig. 3 for all values of T_R.

6. Discussion and conclusions

Expressing a general rotation as the product of rotations about the longitudinal and transverse axes, we have shown that any off-resonance pulse is equivalent to an on-resonance pulse with additional precession before and after the pulse. Using this decomposition, the analysis of pulse sequences in inhomogeneous fields can therefore be mapped to the more familiar case of pulse sequences with on-resonance pulses, even if the offset frequency $\delta\omega_0$ is large compared to the RF amplitude ω_1.

In this paper, we have demonstrated this equivalence with a detailed comparison of experimental and theoretical results for the case of SSFP. The magnitude of SSFP echoes generated by a series of off-resonance RF pulses is identical to that of SSFP echoes generated by on-resonance RF pulses with a flip angle that is modified from $\omega_1\tau_p$ to $\alpha_{\text{eff}}(\delta\omega_0\tau_p, \omega_1\tau_p)$, given in Eq. (4). In [13] we have shown that for a given pulse spacing, the flip angle controls the sensitivity of the SSFP pulse sequence

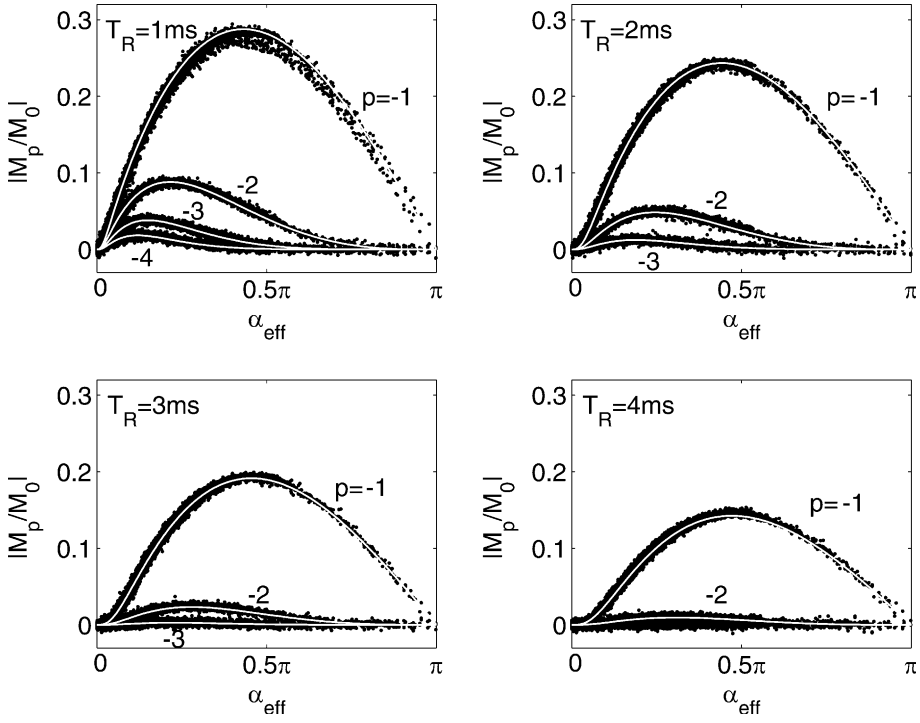

Fig. 4. The measured magnitudes of SSFP echoes in an inhomogeneous field as a function of α_{eff} for four different pulse spacings T_R as indicated in the panels. Increasing the pulse spacing leads to enhanced diffusion effects. In each panel, the experimental data collapse onto distinct curves that are labeled with the respective mode number p. The solid lines are theoretical results based on calculations with on-resonance pulses.

to diffusion effects. For example, for the $p = 0$ mode, the diffusion sensitivity can be described by different diffusion regimes that depend on the size of the flip angle relative to the Ernst angle, α_E, where $\cos\alpha_E = \exp\{-T_R/T_1\}$. The diffusion sensitivity below α_E is weak, vanishes exactly at α_E, and becomes large just above α_E. With an extended sample in a static gradient, the range of Larmor frequencies leads to a large range of effective flip angles α_{eff} across the sample which can span different diffusion regimes. Using a one parameter fit, the magnetization as a function of flip angle can be used to find the diffusion coefficient [12]. The shape of the spectrum therefore encodes directly information on diffusion that can be measured in a simple one-dimensional experiment.

This is an example where large field inhomogeneities can, in principle, lead to a reduction in measurement time. With conventional near-resonance pulses, a 2-D acquisition is required to obtain diffusion information from steady-state sequences [12,17–19]. In contrast, with large inhomogeneities, the same information can be obtained from the spectrum of a 1-D experiment using a single fixed value of B_1.

The equivalence concept presented in this paper is very general: to any pulse sequence with off-resonance pulses, including composite or shaped pulses, there is an equivalent sequence with on-resonance pulses that has exactly the same spin dynamics, including diffusion and relaxation effects. The scheme is particularly powerful for sequences with a large number of equivalent pulses, such as the SSFP or DANTE [20] sequences. In such cases, the modified sequences are closely related to the original sequences: the frequency offset is mapped to a rescaling of the pulse amplitudes. In sequences with more than one type of pulse, the pulse amplitude and phase of each inequivalent pulse is rescaled differently, since α_{eff} and η are not linear functions of the tipping angle $\omega_1\tau_p$. As an example, the Carr–Purcell–Meiboom–Gill (CPMG) sequence consists of two types of inequivalent pulses, the initial 90° pulse and the following 180° pulses. The off-resonance behavior of the CPMG sequence can then be understood by mapping it onto the equivalent on-resonance sequence. The resulting magnetization can be written as a weighted sum of the responses to on-resonance CPMG and Carr–Purcell (CP) sequences with identical misset 180° pulses. This gives rise to the enhanced diffusion sensitivity of the CPMG sequence with off-resonance pulses [21].

References

[1] R.L. Kleinberg, in: Encyclopedia of Nuclear Magnetic Resonance, vol. 8, Wiley, Chichester, 1996, pp. 4960–4969, Chapter: Well logging.

[2] G. Eidmann, R. Savelsberg, P. Blümler, B. Blümich, The NMR MOUSE, a mobile universal surface explorer, J. Magn. Reson. A 122 (1996) 104–109.

[3] R. Kimmich, E. Fischer, One- and two-dimensional pulse sequences for diffusion experiments in the fringe field of superconducting magnets, J. Magn. Reson. A 106 (1994) 229–235.

[4] P.J. McDonald, Stray field magnetic resonance imaging, Prog. Nucl. Magn. Reson. Spect. 30 (1997) 69–99.

[5] C.A. Meriles, D. Sakellariou, H. Heise, A.J. Moulé, A. Pines, Approach to high-resolution ex situ NMR spectroscopy, Science 293 (2001) 82–85.

[6] E.T. Jaynes, Matrix treatment of nuclear induction, Phys. Rev. 98 (1955) 1099–1105.

[7] A.L. Bloom, Nuclear induction in inhomogeneous fields, Phys. Rev. 98 (1955) 1105–1111.

[8] R. Bradford, C. Clay, E. Strick, A steady-state transient technique in nuclear induction, Phys. Rev. 84 (1951) 157–158.

[9] H.Y. Carr, Steady-state free precession in nuclear magnetic resonance, Phys. Rev. 112 (1958) 1693–1701.

[10] R. Kaiser, E. Bartholdi, R.R. Ernst, Diffusion and field-gradient effects in NMR Fourier spectroscopy, J. Chem. Phys. 60 (1974) 2966–2979.

[11] S. Patz, R.C. Hawkes, The application of steady-state free precession to the study of very slow fluid flow, Magn. Reson. Med. 3 (1986) 140–145.

[12] R.B. Buxton, The diffusion sensitivity of fast steady-state free precession imaging, Magn. Reson. Med. 29 (1993) 235–243.

[13] D.E. Freed, U.M. Scheven, L.J. Zielinski, P.N. Sen, M.D. Hürlimann, Steady-state free precession experiments and exact treatment of diffusion in a uniform gradient, J. Chem. Phys. 115 (2001) 4249–4258.

[14] M.E. Rose, Elementary Theory of Angular Momentum, Wiley, New York, 1957.

[15] C. Counsell, M.H. Levitt, R.R. Ernst, Analytical theory of composite pulses, J. Magn. Reson. 63 (1985) 133–141.

[16] Y. Zur, E. Bosak, N. Kaplan, Motion-insensitive, steady state free precession imaging, Magn. Reson. Med. 37 (1997) 716–722.

[17] K.D. Merboldt, W. Hänicke, M.L. Gyngell, J. Frahm, H. Bruhn, Rapid NMR imaging of molecular self-diffusion using a modified CE-FAST sequence, J. Magn. Reson. 82 (1989) 115–121.

[18] D. Le Bihan, R. Turner, J.R. Macfall, Effects of intravoxel incoherent motions (IVIM) in steady-state free precession (SSFP) imaging: application to molecular diffusion imaging, Magn. Reson. Med. 10 (1989) 324–337.

[19] Y. Zur, E. Bosak, N. Kaplan, A new diffusion SSFP imaging technique, Magn. Reson. Med. 37 (1997) 716–722.

[20] G.A. Morris, R. Freeman, Selective excitation in Fourier transform nuclear magnetic resonance, J. Magn. Reson. 29 (1978) 433–462.

[21] M.D. Hürlimann, Diffusion and relaxation effects in general stray field NMR experiments, J. Magn. Reson. 148 (2001) 367–378.